Figure S1

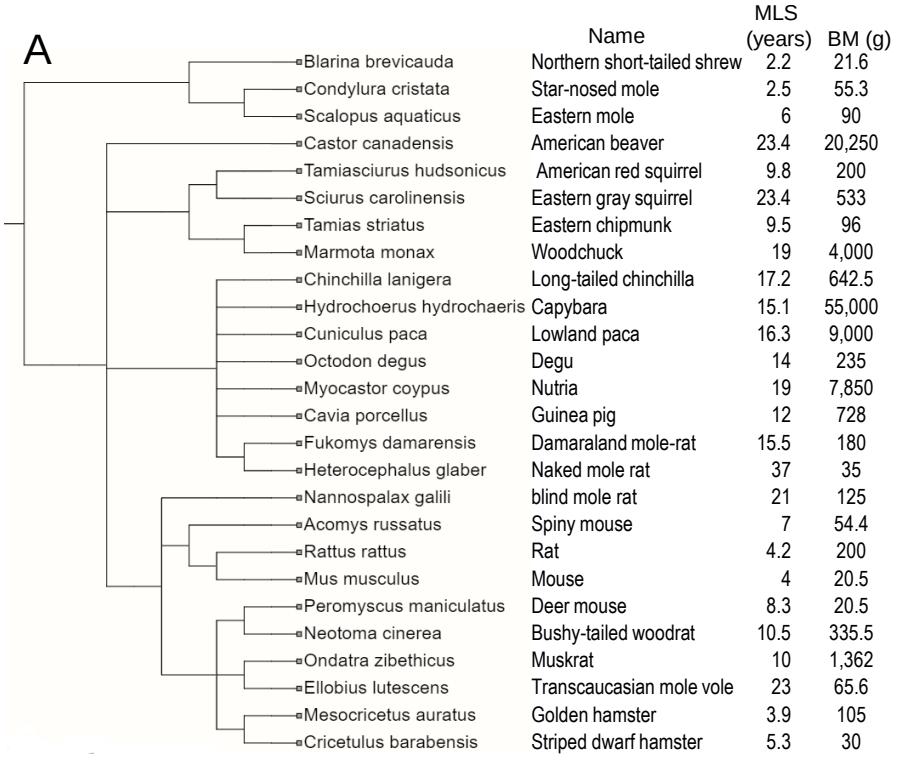
A
Name
MLS (years)
BM (g)
Blarina brevicauda Northern short-tailed shrew 2.2 21.6
Condylura cristata Star-nosed mole 2.5 55.3
Scalopus aquaticus Eastern mole 6 90
Castor canadensis American beaver 23.4 20,250
Tamiasciurus hudsonicus American red squirrel 9.8 200
Sciurus carolinensis Eastern gray squirrel 23.4 533
Tamias striatus Eastern chipmunk 9.5 96
Marmota monax Woodchuck 19 4,000
Chinchilla lanigera Long-tailed chinchilla 17.2 642.5
Hydrochoerus hydrochaeris Capybara 15.1 55,000
Cuniculus paca Lowland paca 16.3 9,000
Octodon degus Degu 14 235
Myocastor coypus Nutria 19 7,850
Cavia porcellus Guinea pig 12 728
Fukomys damarensis Damaraland mole-rat 15.5 180
Heterocephalus glaber Naked mole rat 37 35
Nannospalax galili blind mole rat 21 125
Acomys russatus Spiny mouse 7 54.4
Rattus rattus Rat 4.2 200
Mus musculus Mouse 4 20.5
Peromyscus maniculatus Deer mouse 8.3 20.5
Neotoma cinerea Bushy-tailed woodrat 10.5 335.5
Ondatra zibethicus Muskrat 10 1,362
Ellobius lutescens Transcaucasian mole vole 23 65.6
Mesocricetus auratus Golden hamster 3.9 105
Cricetulus barabensis Striped dwarf hamster 5.3 30

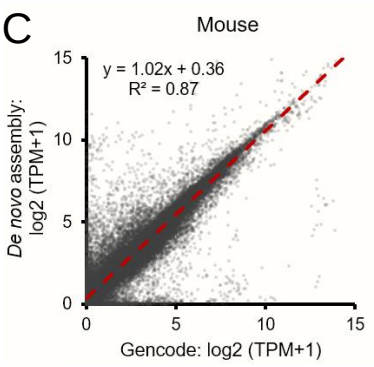
C
Mouse
y = 1.02x + 0.36
R² = 0.87
De novo assembly: log2 (TPM+1)
Gencode: log2 (TPM+1)

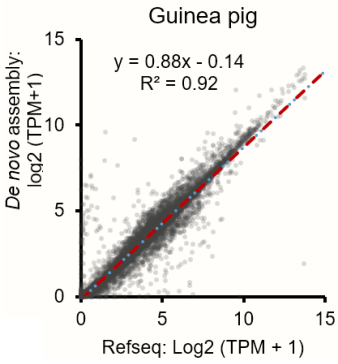
Guinea pig
y = 0.88x - 0.14
R² = 0.92
De novo assembly: log2 (TPM+1)
Refseq: Log2 (TPM + 1)

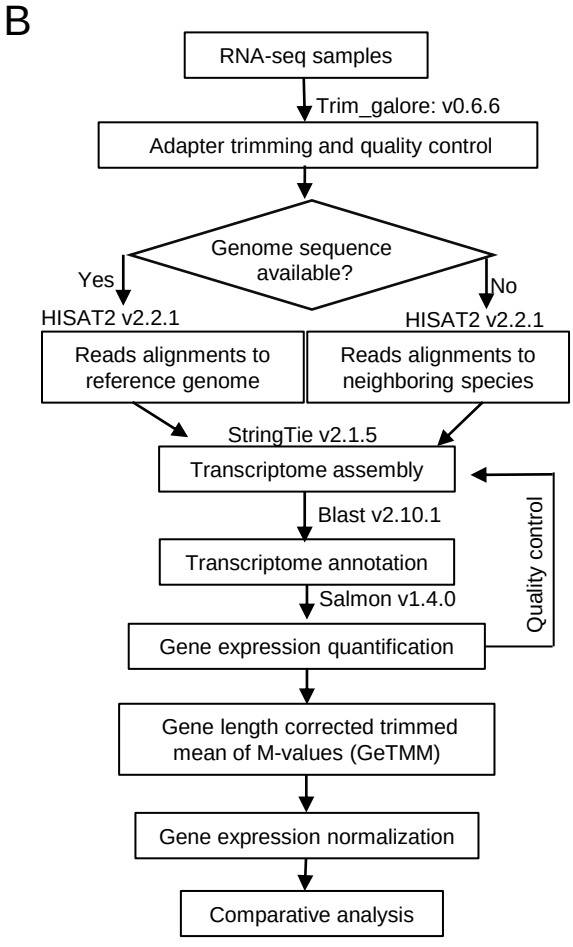
B
RNA-seq samples
Trim_galore: v0.6.6
Adapter trimming and quality control
Genome sequence available?
Yes
No
HISAT2 v2.2.1
HISAT2 v2.2.1
Reads alignments to reference genome
Reads alignments to neighboring species
StringTie v2.1.5
Transcriptome assembly
Blast v2.10.1
Transcriptome annotation
Salmon v1.4.0
Gene expression quantification
Quality control
Gene length corrected trimmed mean of M-values (GeTMM)
Gene expression normalization
Comparative analysis

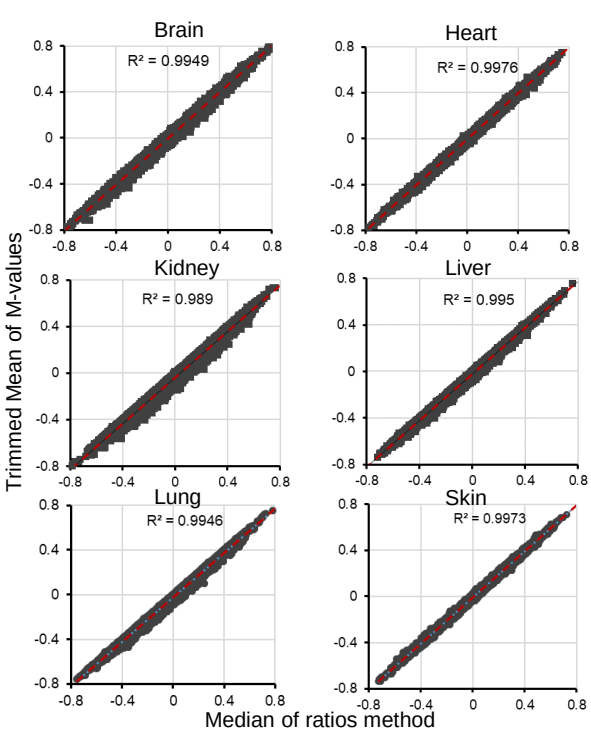
D
Brain
R² = 0.9949
Heart
R² = 0.9976
Kidney
R² = 0.989
Liver
R² = 0.995
Lung
R² = 0.9946
Skin
R² = 0.9973
Trimmed Mean of M-values
Median of ratios method

Figure S1. Workflow of comparative transcriptomics and quality control. Related to Figure 1.

(A) A phylogenetic tree of species used in this study. Corresponding MLS and body mass are also shown.

(B) Workflow showing the comparative transcriptomics.

(C) Scatter plots showing the comparison of gene expression from *de novo* transcriptome assembly in this study (y-axis) and public Gencode or Refseq annotations (x-axis). Mouse and guinea pig are shown as examples. Transcript per million (TPM) was used to represent the relative gene expression levels.

(D) Scatter plots showing the comparison of normalization methods including Median of ratios method (x-axis) and trimmed mean of M-values (y-axis). High consistency between the two methods was observed.

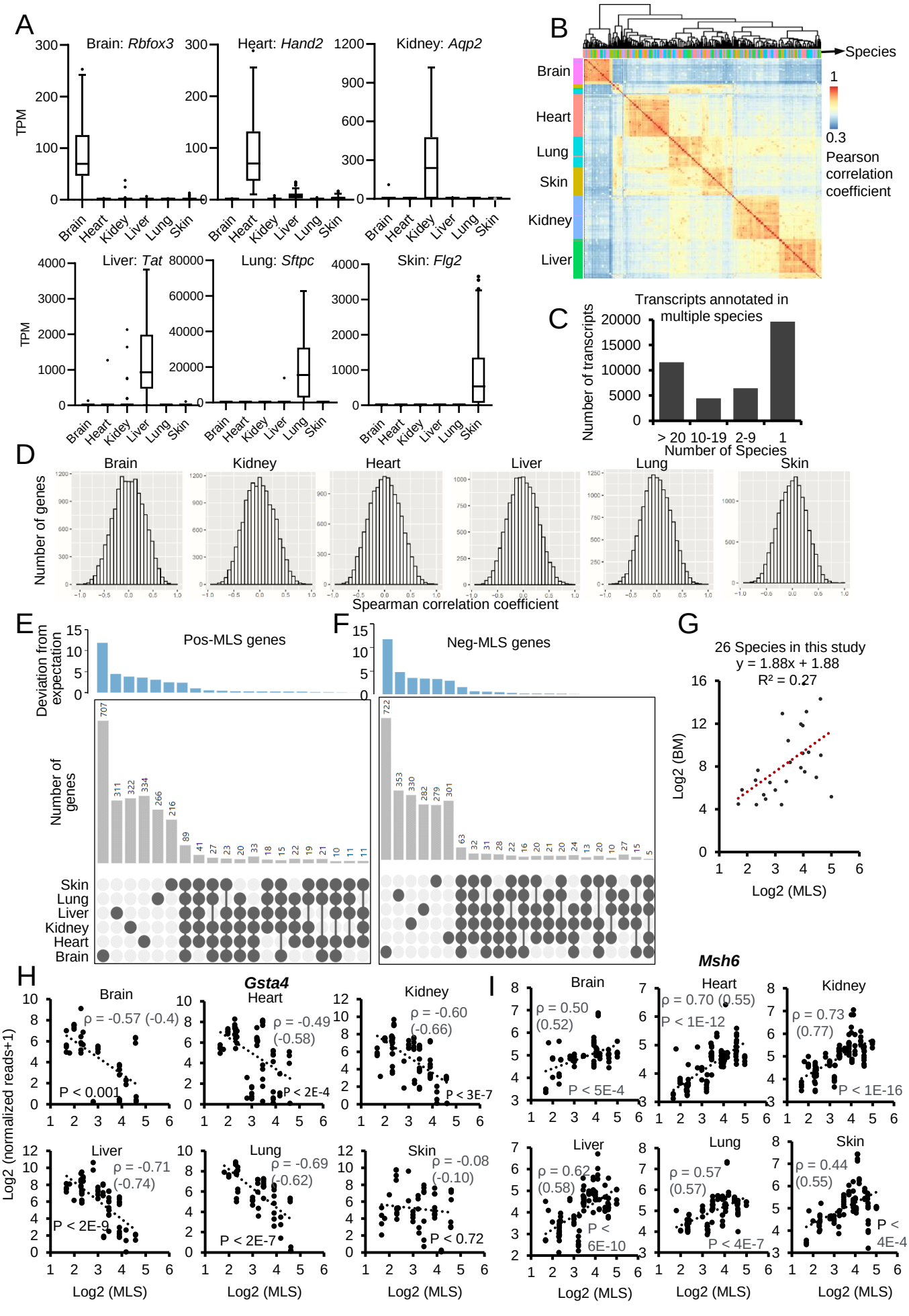
A
Brain: Rbfox3
Heart: Hand2
Kidney: Aqp2
Liver: Tat
Lung: Sftpc
Skin: Flg2
TPM
Brain
Heart
Kidey
Liver
Lung
Skin
B
Species
Pearson correlation coefficient
C
Transcripts annotated in multiple species
Number of transcripts
> 20
10-19
2-9
1
Number of Species
D
Number of genes
Spearman correlation coefficient
E
Pos-MLS genes
Deviation from expectation
Number of genes
F
Neg-MLS genes
G
26 Species in this study
y = 1.88x + 1.88
R² = 0.27
Log2 (BM)
Log2 (MLS)
H
Gsta4
Log2 (normalized reads+1)
Log2 (MLS)
I
Msh6

Figure S2. Overlap of Pos- and Neg-MLS genes identified in 6 tissues. Related to Figure 1.

(A) Boxplots showing the gene expression of tissue-specific marker genes in six tissues.

(B) Hierarchical clustering of all RNA-seq samples. Samples were clustered by tissues instead of species.

(C) The barplot showing the number of homologous genes that can be identified across species. The x-axis indicates the number of species. The y-axis indicates the number of homologous transcripts.

(D) Histogram plots showing the distribution of Spearman correlation coefficients between gene expression and MLS.

(E-F) Upset plots showing the overlap of Pos-MLS (E) and Neg-MLS (F) genes identified in 6 tissues. The categories were ranked by deviations from the expected cardinality.

(G) The scatter plot showing the correlation of MLS (years) and body mass (g).

(H-I) Scatter plots showing the relative gene expression level of *Gsta4* (H) and *Msh6* (I) in six tissues across species with different MLS. Spearman correlation coefficients (ρ) of gene expression and MLS are also shown. Phylogenetically corrected values for ρ are shown in parenthesis.

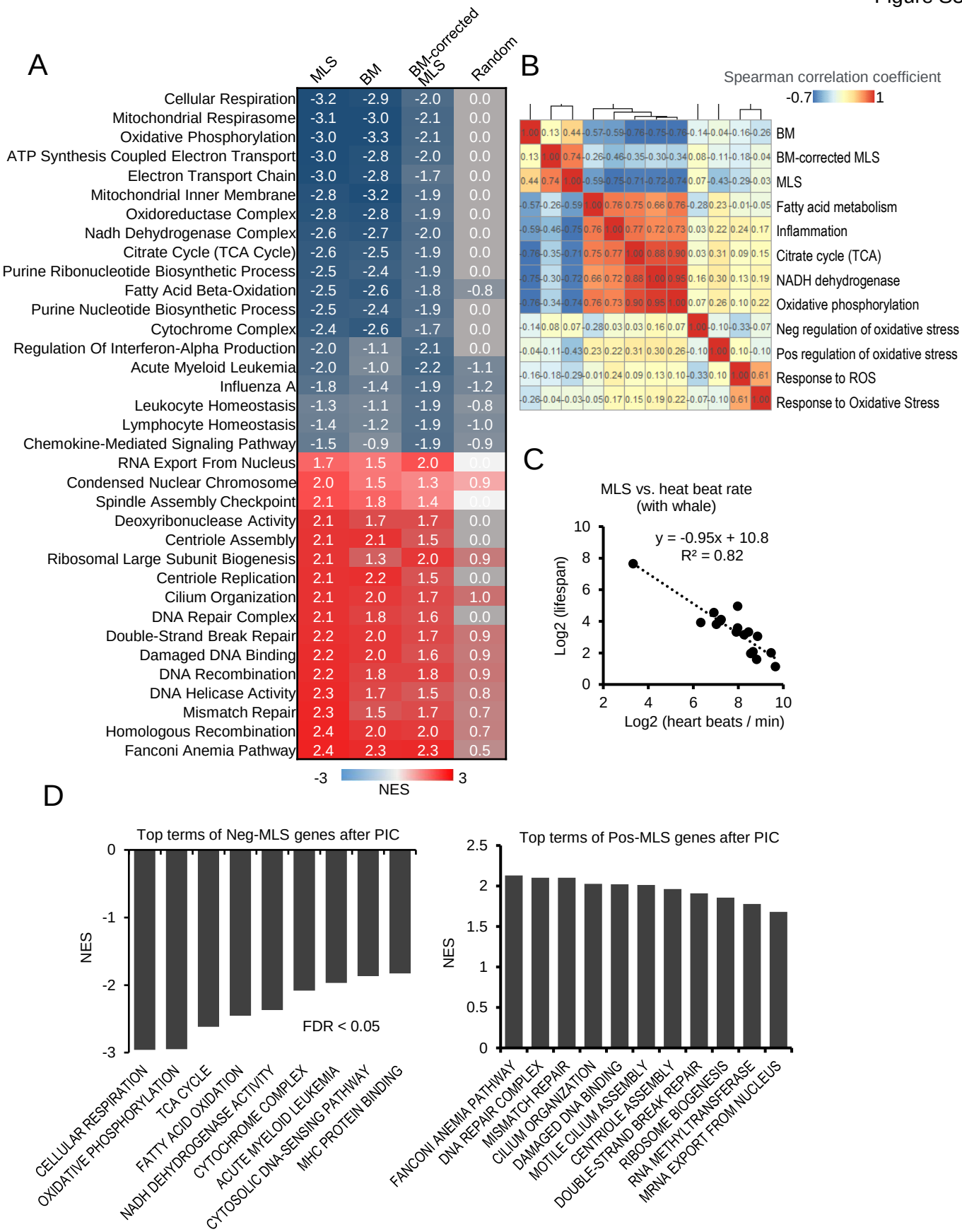
A
MLS
BM
BM-corrected MLS
Random
Cellular Respiration -3.2 -2.9 -2.0 0.0
Mitochondrial Respirasome -3.1 -3.0 -2.1 0.0
Oxidative Phosphorylation -3.0 -3.3 -2.1 0.0
ATP Synthesis Coupled Electron Transport -3.0 -2.8 -2.0 0.0
Electron Transport Chain -3.0 -2.8 -1.7 0.0
Mitochondrial Inner Membrane -2.8 -3.2 -1.9 0.0
Oxidoreductase Complex -2.8 -2.8 -1.9 0.0
Nadh Dehydrogenase Complex -2.6 -2.7 -2.0 0.0
Citrate Cycle (TCA Cycle) -2.6 -2.5 -1.9 0.0
Purine Ribonucleotide Biosynthetic Process -2.5 -2.4 -1.9 0.0
Fatty Acid Beta-Oxidation -2.5 -2.6 -1.8 -0.8
Purine Nucleotide Biosynthetic Process -2.5 -2.4 -1.9 0.0
Cytochrome Complex -2.4 -2.6 -1.7 0.0
Regulation Of Interferon-Alpha Production -2.0 -1.1 -2.1 0.0
Acute Myeloid Leukemia -2.0 -1.0 -2.2 -1.1
Influenza A -1.8 -1.4 -1.9 -1.2
Leukocyte Homeostasis -1.3 -1.1 -1.9 -0.8
Lymphocyte Homeostasis -1.4 -1.2 -1.9 -1.0
Chemokine-Mediated Signaling Pathway -1.5 -0.9 -1.9 -0.9
RNA Export From Nucleus 1.7 1.5 2.0 0.0
Condensed Nuclear Chromosome 2.0 1.5 1.3 0.9
Spindle Assembly Checkpoint 2.1 1.8 1.4 0.0
Deoxyribonuclease Activity 2.1 1.7 1.7 0.0
Centriole Assembly 2.1 2.1 1.5 0.0
Ribosomal Large Subunit Biogenesis 2.1 1.3 2.0 0.9
Centriole Replication 2.1 2.2 1.5 0.0
Cilium Organization 2.1 2.0 1.7 1.0
DNA Repair Complex 2.1 1.8 1.6 0.0
Double-Strand Break Repair 2.2 2.0 1.7 0.9
Damaged DNA Binding 2.2 2.0 1.6 0.9
DNA Recombination 2.2 1.8 1.8 0.9
DNA Helicase Activity 2.3 1.7 1.5 0.8
Mismatch Repair 2.3 1.5 1.7 0.7
Homologous Recombination 2.4 2.0 2.0 0.7
Fanconi Anemia Pathway 2.4 2.3 2.3 0.5
-3
NES
3
B
Spearman correlation coefficient
-0.7
1
BM
BM-corrected MLS
MLS
Fatty acid metabolism
Inflammation
Citrate cycle (TCA)
NADH dehydrogenase
Oxidative phosphorylation
Neg regulation of oxidative stress
Pos regulation of oxidative stress
Response to ROS
Response to Oxidative Stress
C
MLS vs. heat beat rate
(with whale)
y = -0.95x + 10.8
R² = 0.82
Log2 (lifespan)
Log2 (heart beats / min)
D
Top terms of Neg-MLS genes after PIC
NES
FDR < 0.05
CELLULAR RESPIRATION
OXIDATIVE PHOSPHORYLATION
TCA CYCLE
FATTY ACID OXIDATION
NADH DEHYDROGENASE ACTIVITY
CYTOCHROME COMPLEX
ACUTE MYELOID LEUKEMIA
CYTOSOLIC DNA-SENSING PATHWAY
MHC PROTEIN BINDING
Top terms of Pos-MLS genes after PIC
NES
FANCONI ANEMIA PATHWAY
DNA REPAIR COMPLEX
MISMATCH REPAIR
CILIUM ORGANIZATION
DAMAGED DNA BINDING
MOTILE CILIUM ASSEMBLY
CENTRIOLE ASSEMBLY
DOUBLE-STRAND BREAK REPAIR
RIBOSOME BIOGENESIS
RNA METHYLTRANSFERASE
MRNA EXPORT FROM NUCLEUS

Figure S3. GSEA with gene expression after correction for BM and phylogenetically independent contrasts. Related to Figures 2-3.

(A) Heatmap plot showing the normalized enrichment scores of GSEA with genes ranked by the Spearman correlation coefficients of gene expression with BM, MLS and BM-corrected MLS, respectively.

(B) Hierarchical clustering based on average gene expression of Neg-MLS involved in different categories. The numbers shown in the heatmap are Spearman correlation coefficients. Genes used for each category were from GO and KEGG. NADH dehydrogenase: GO_0010257 and GO_0003954; Fatty acid metabolism: GO_0019395; Oxidative phosphorylation: GO_0006119; Citrate cycle (TCA): map00020; Cellular response to reactive oxygen species: GO_0034614; Cellular response to oxidative stress : GO_0034599; Negative regulation of response to oxidative stress: GO_1902883; Positive regulation of response to oxidative stress: GO_1902884; Inflammation: GO_0002526, GO_0002260, GO_0001776, GO_0032647 and GO_0070098.

(C) Scatter plot showing the relationship of heartbeat rate and MLS across species.

(D) Top enriched terms identified by GSEA with Neg-MLS (left) and Pos-MLS (right) gene expression after phylogenetically independent contrasts as inputs.

Figure S4

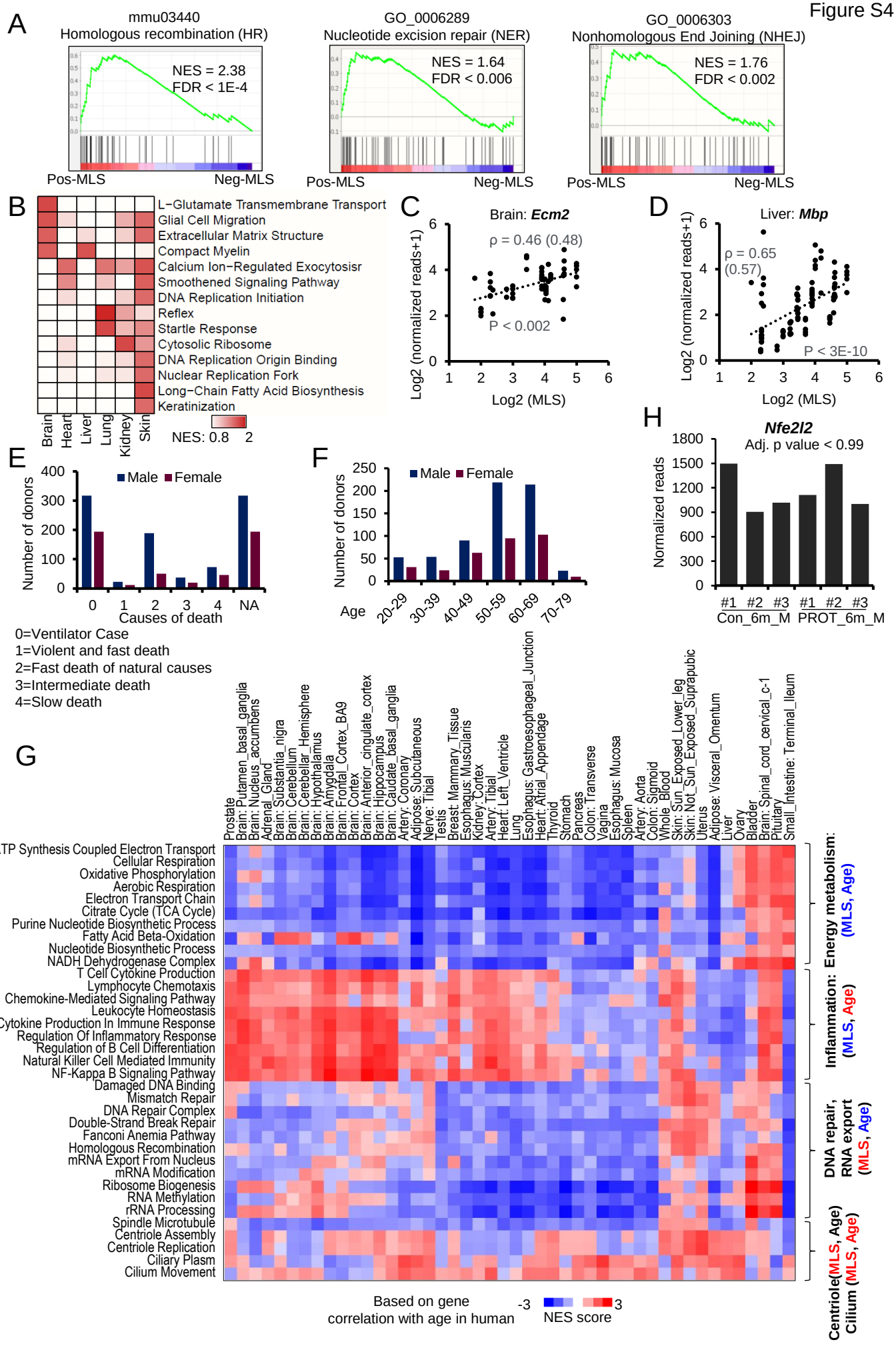
A
mmu03440
Homologous recombination (HR)
NES = 2.38
FDR < 1E-4
Pos-MLS
Neg-MLS
GO_0006289
Nucleotide excision repair (NER)
NES = 1.64
FDR < 0.006
Pos-MLS
Neg-MLS
GO_0006303
Nonhomologous End Joining (NHEJ)
NES = 1.76
FDR < 0.002
Pos-MLS
Neg-MLS
B
L−Glutamate Transmembrane Transport
Glial Cell Migration
Extracellular Matrix Structure
Compact Myelin
Calcium Ion−Regulated Exocytosisr
Smoothened Signaling Pathway
DNA Replication Initiation
Reflex
Startle Response
Cytosolic Ribosome
DNA Replication Origin Binding
Nuclear Replication Fork
Long−Chain Fatty Acid Biosynthesis
Keratinization
Brain
Heart
Liver
Lung
Kidney
Skin
NES: 0.8 2
C
Brain: Ecm2
ρ = 0.46 (0.48)
P < 0.002
Log2 (normalized reads+1)
Log2 (MLS)
D
Liver: Mbp
ρ = 0.65
(0.57)
P < 3E-10
Log2 (normalized reads+1)
Log2 (MLS)
E
Male
Female
Number of donors
Causes of death
0
1
2
3
4
NA
0=Ventilator Case
1=Violent and fast death
2=Fast death of natural causes
3=Intermediate death
4=Slow death
F
Male
Female
Number of donors
Age
20-29
30-39
40-49
50-59
60-69
70-79
H
Nfe2l2
Adj. p value < 0.99
Normalized reads
#1 #2 #3 #1 #2 #3
Con_6m_M PROT_6m_M
G
Prostate
Brain: Putamen_basal_ganglia
Brain: Nucleus_accumbens
Adrenal_Gland
Brain: Substantia_nigra
Brain: Cerebellum
Brain: Cerebellar_Hemisphere
Brain: Hypothalamus
Brain: Amygdala
Brain: Frontal_Cortex_BA9
Brain: Cortex
Brain: Anterior_cingulate_cortex
Brain: Hippocampus
Brain: Caudate_basal_ganglia
Artery: Coronary
Adipose: Subcutaneous
Nerve: Tibial
Testis
Breast: Mammary_Tissue
Esophagus: Muscularis
Kidney: Cortex
Artery: Tibial
Heart: Left_Ventricle
Lung
Esophagus: Gastroesophageal_Junction
Heart: Atrial_Appendage
Thyroid
Stomach
Pancreas
Colon: Transverse
Vagina
Esophagus: Mucosa
Spleen
Artery: Aorta
Colon: Sigmoid
Whole_Blood
Skin: Sun_Exposed_Lower_leg
Skin: Not_Sun_Exposed_Suprapubic
Uterus
Adipose: Visceral_Omentum
Liver
Ovary
Bladder
Brain: Spinal_cord_cervical_c-1
Pituitary
Small_Intestine: Terminal_Ileum
ATP Synthesis Coupled Electron Transport
Cellular Respiration
Oxidative Phosphorylation
Aerobic Respiration
Electron Transport Chain
Citrate Cycle (TCA Cycle)
Purine Nucleotide Biosynthetic Process
Fatty Acid Beta-Oxidation
Nucleotide Biosynthetic Process
NADH Dehydrogenase Complex
T Cell Cytokine Production
Lymphocyte Chemotaxis
Chemokine-Mediated Signaling Pathway
Leukocyte Homeostasis
Cytokine Production In Immune Response
Regulation Of Inflammatory Response
Regulation of B Cell Differentiation
Natural Killer Cell Mediated Immunity
NF-Kappa B Signaling Pathway
Damaged DNA Binding
Mismatch Repair
DNA Repair Complex
Double-Strand Break Repair
Fanconi Anemia Pathway
Homologous Recombination
mRNA Export From Nucleus
mRNA Modification
Ribosome Biogenesis
RNA Methylation
rRNA Processing
Spindle Microtubule
Centriole Assembly
Centriole Replication
Ciliary Plasm
Cilium Movement
Energy metabolism: (MLS, Age)
Inflammation: (MLS, Age)
DNA repair, RNA export (MLS, Age)
Centriole(MLS, Age) Cilium (MLS, Age)
Based on gene correlation with age in human
-3
3
NES score

Figure S4. Expression of MLS-associated genes during human aging. Related to Figure 3.

(A) GSEA plots showing global enrichment of representative GO or KEGG terms including mmu03440_Homologous recombination, GO_0006289_Nucleotide excision repair and nonhomologous end joining. NES and FDR values are shown in the plots.

(B) The heatmap showing the tissues-specific functional terms that Pos-MLS genes are enriched in. Colors indicate NES values from GSEA in each tissue. Functional terms enriched across all tissues (Figure 3A) are not shown to avoid redundancy.

(C-D) Scatter plots showing the relative expression level of *Ecm2* (C) and *Mbp* (D) in the brain and liver across species.

(E) Cause of death distribution of donors for human gene expression data from GTEx.

(F) Age distribution of donors for human gene expression data from GTEx.

(G) The heatmap showing NES of MLS-associated pathways based on the correlation of gene expression with age. Negative NES values shown in Blue indicate expression of genes involved in this pathway tend to negatively correlate with age, i.e. downregulated during human aging. Positive NES values shown in Red indicate expression of genes involved in this pathway tend to positively correlate with age, i.e. upregulated during human aging. Gene expression data is from GTEx.

(H) Barplot showing the relative expression of *Nfe2l2* in the control mice and mice treated with Protandim (tissue: Liver; dose: 1200 ppm; duration: 2 months). RNA-seq data was from GSE131901.

Figure S5

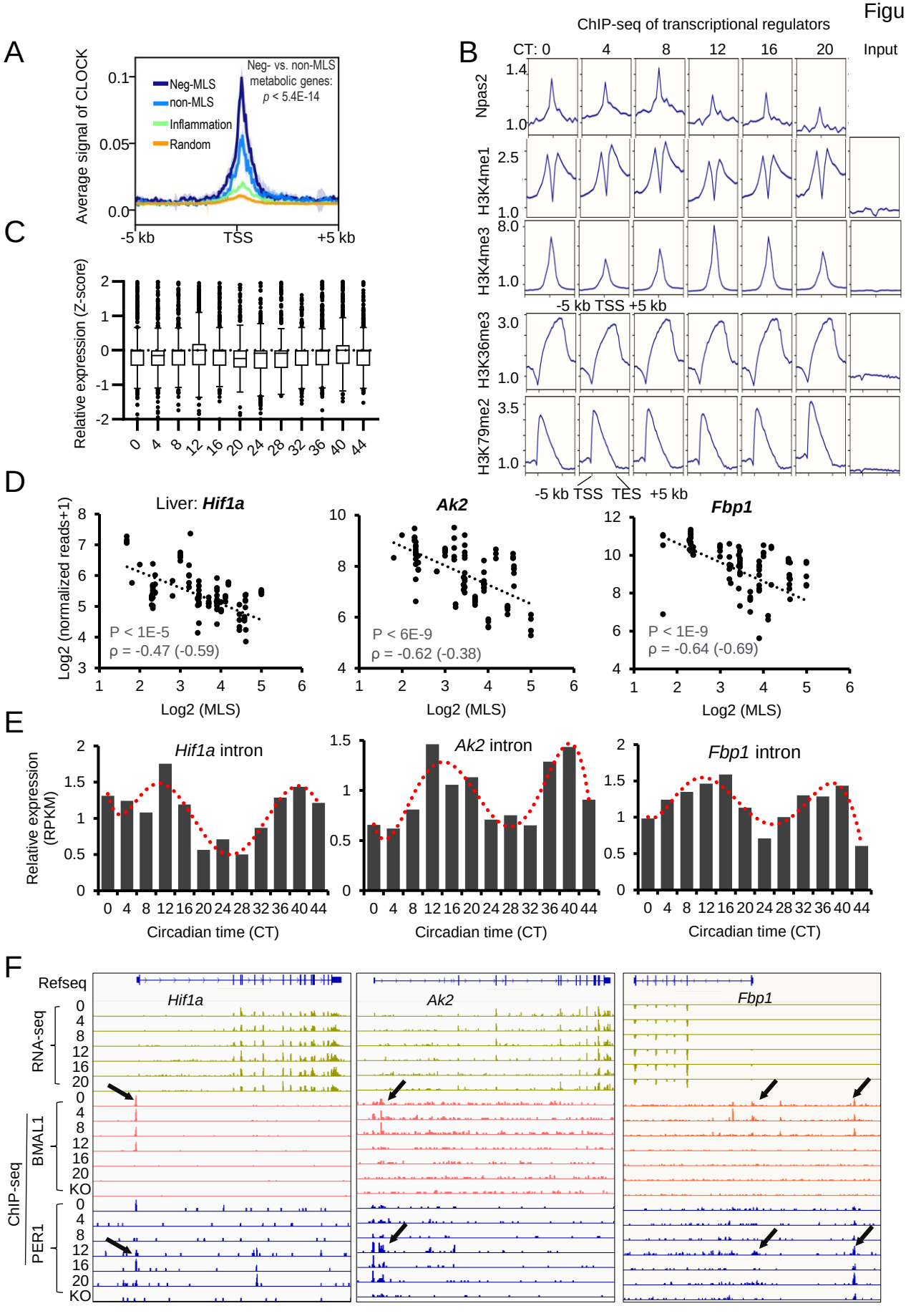
A
Average signal of CLOCK
Neg-MLS
non-MLS
Inflammation
Random
Neg- vs. non-MLS metabolic genes: p < 5.4E-14
-5 kb
TSS
+5 kb
B
ChIP-seq of transcriptional regulators
CT: 0 4 8 12 16 20 Input
Npas2
H3K4me1
H3K4me3
H3K36me3
H3K79me2
-5 kb TSS +5 kb
-5 kb TSS TES +5 kb
C
Relative expression (Z-score)
D
Liver: Hif1a
Ak2
Fbp1
Log2 (normalized reads+1)
P < 1E-5
ρ = -0.47 (-0.59)
P < 6E-9
ρ = -0.62 (-0.38)
P < 1E-9
ρ = -0.64 (-0.69)
Log2 (MLS)
E
Hif1a intron
Ak2 intron
Fbp1 intron
Relative expression (RPKM)
Circadian time (CT)
F
Refseq
Hif1a
Ak2
Fbp1
RNA-seq
ChIP-seq
BMAL1
PER1
KO

Figure S5. Transcriptomic and epigenomic signatures of Neg-MLS genes during circadian cycle. Related to Figure 5.

(A) Metagene analysis showing differential binding activities of circadian regulator CLOCK in mouse liver at Neg-MLS gene involved in cellular respiratory based energy metabolism or inflammation, and metabolic genes that correlated with MLS or not. Five kb around the TSS regions are shown. Genes involved in cellular respiratory-based energy metabolism were identified in Figure S3B. Liver ChIP-seq data is from (Annayev et al., 2014).

(B) Metagene analysis showing dynamic binding activities of circadian regulator Npas2 and histone modifications at Neg-MLS genes in mouse liver. Five kb around the TSS regions are shown for H3K4me1 and H3K4me3. Five kb around the TSS and TES regions are shown for late and early elongation histone modification markers H3K36me3 and H3K79me2. ChIP-seq data is from (Koike et al., 2012).

(C) Boxplots showing the dynamic transcriptional activity of random genes with low circadian factor binding in two circadian cycles. CT, circadian time. All genes were ranked by their TSS occupancy of circadian factors and genes shown in boxplot were randomly selected from genes with a lower 50% of circadian factors binding. All MLS-associated genes are excluded.

(D) Scatter plots showing the relative gene expression levels of *Hif1a* (left), *Ak2* (middle) and *Fbp1* (right) in the liver across species with different MLS. Spearman correlation coefficients (ρ) of gene expression and MLS are shown. Phylogenetically corrected values for ρ are shown in parenthesis.

(E) The barplots showing the dynamic transcription of *Hif1a* (left), *Ak2* (middle) and *Fbp1* (right) genes in two circadian cycles.

(F) Tracks of *Hif1a* (left), *Ak2* (middle) and *Fbp1* (right) genomic regions. The RNA-seq and ChIP-seq of BMAL1 (activator) and PER1 (repressor) are shown. The arrows highlight the binding sites of BMAL1 and PER1. RNA-seq and ChIP-seq are from (Koike et al., 2012).

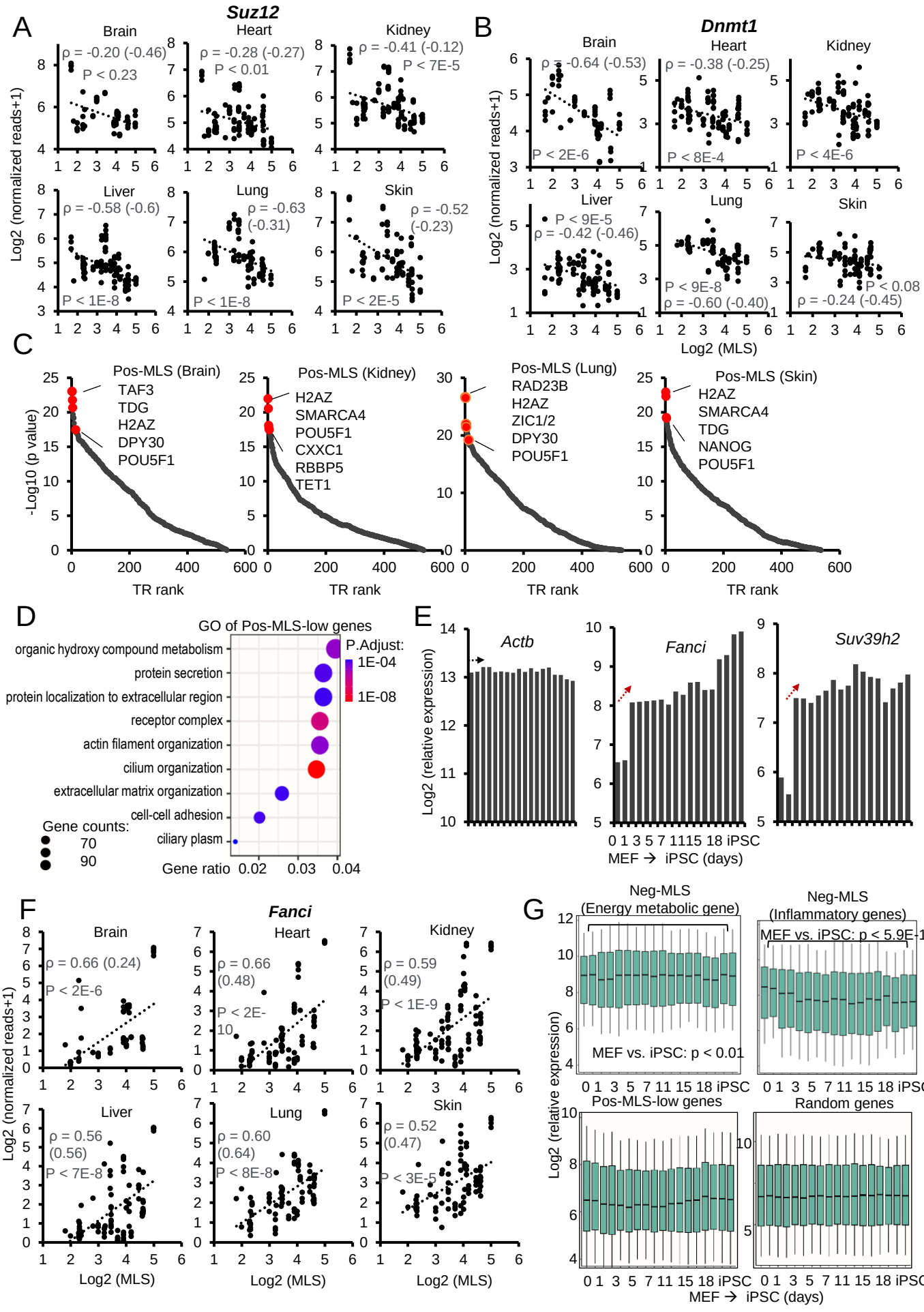
A
Suz12
Brain
ρ = -0.20 (-0.46)
P < 0.23
Heart
ρ = -0.28 (-0.27)
P < 0.01
Kidney
ρ = -0.41 (-0.12)
P < 7E-5
Liver
ρ = -0.58 (-0.6)
P < 1E-8
Lung
ρ = -0.63 (-0.31)
P < 1E-8
Skin
ρ = -0.52 (-0.23)
P < 2E-5
Log2 (normalized reads+1)
B
Dnmt1
Brain
ρ = -0.64 (-0.53)
P < 2E-6
Heart
ρ = -0.38 (-0.25)
P < 8E-4
Kidney
P < 4E-6
Liver
P < 9E-5
ρ = -0.42 (-0.46)
Lung
P < 9E-8
ρ = -0.60 (-0.40)
Skin
P < 0.08
ρ = -0.24 (-0.45)
Log2 (normalized reads+1)
Log2 (MLS)
C
-Log10 (p value)
Pos-MLS (Brain)
TAF3
TDG
H2AZ
DPY30
POU5F1
Pos-MLS (Kidney)
H2AZ
SMARCA4
POU5F1
CXXC1
RBBP5
TET1
Pos-MLS (Lung)
RAD23B
H2AZ
ZIC1/2
DPY30
POU5F1
Pos-MLS (Skin)
H2AZ
SMARCA4
TDG
NANOG
POU5F1
TR rank
D
GO of Pos-MLS-low genes
organic hydroxy compound metabolism
protein secretion
protein localization to extracellular region
receptor complex
actin filament organization
cilium organization
extracellular matrix organization
cell-cell adhesion
ciliary plasm
P.Adjust:
1E-04
1E-08
Gene counts:
70
90
Gene ratio
E
Actb
Fanci
Suv39h2
Log2 (relative expression)
0 1 3 5 7 1115 18 iPSC
MEF → iPSC (days)
F
Fanci
Brain
ρ = 0.66 (0.24)
P < 2E-6
Heart
ρ = 0.66 (0.48)
P < 2E-10
Kidney
ρ = 0.59 (0.49)
P < 1E-9
Liver
ρ = 0.56 (0.56)
P < 7E-8
Lung
ρ = 0.60 (0.64)
P < 8E-8
Skin
ρ = 0.52 (0.47)
P < 3E-5
Log2 (normalized reads+1)
Log2 (MLS)
G
Neg-MLS (Energy metabolic gene)
MEF vs. iPSC: p < 0.01
Neg-MLS (Inflammatory genes)
MEF vs. iPSC: p < 5.9E-11
Pos-MLS-low genes
Random genes
Log2 (relative expression)
0 1 3 5 7 11 15 18 iPSC
MEF → iPSC (days)

Figure S6. Upregulation of Pos-MLS genes during somatic cell reprogramming. Related to Figure 6.

(A-B) Scatter plots showing the relative gene expression level of *Suz12* (A) in PRC2 complex and *Dnmt1*(B) the liver across species. Spearman correlation coefficients (ρ) of gene expression and MLS were shown. Phylogenetically corrected values for ρ are shown in parenthesis.

(C) Scatter plots showing the TR rank of Pos-MLS genes in the brain, kidney, lung and skin. The Y-axis indicates the *p* values that are calculated using the Wilcoxon rank test comparison of the Pos-MLS genes and background. Top regulators with the lowest *p* values are highlighted in red.

(D) The dot plot showing the GO enrichment of genes in the Pos-MLS-low clusters. The colors indicate the BH-adjusted *p* values. The dot sizes indicate the number of genes.

(E) Barplots showing the relative expression of *Actb* (left), *Fanci* (middle) and *Suv39h2* (right) genes during the OSKM-induced somatic reprogramming. Log2 scale of the intensity in CHIP array is shown. Arrows indicate the direction of change in gene expression.

(F) Scatter plots showing the relative gene expression levels of *Fanci* in the six tissues across species. Spearman correlation coefficients (ρ) of gene expression and MLS are shown. Phylogenetically corrected values for ρ are shown in parenthesis.

(G) Boxplot showing the expression of Neg-MLS (up) genes, Pos-MLS-low genes (bottom) and random genes (bottom) during the OSKM-induced somatic reprogramming. p values are calculated using two-tailed Student's t-test. RNA-seq data are from (Chen et al., 2016).

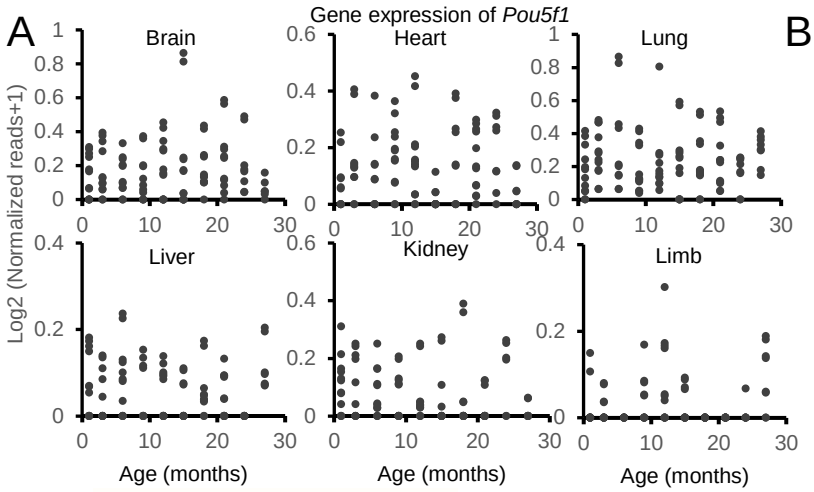

B

Correlation of gene expression with age

	Pou5f1	Nanog	Klf4	Sox2	Myc
BAT	0.20	0.03	0.19	0.02	-0.05
Bone	0.08	0.00	-0.18	0.28	-0.25
Brain	0.07	0.09	0.05	-0.06	0.05
GAT	-0.08	0.39	0.11	0.11	-0.29
Heart	0.00	0.11	-0.22	-0.02	0.02
Kidney	-0.24	-0.03	0.05	0.16	0.20
Limb	0.06	0.18	-0.19	0.02	-0.15
Liver	-0.05	0.13	0.29	0.02	0.01
Lung	0.05	0.22	0.06	0.08	0.27
Marrow	-0.08	-0.05	-0.11	-0.11	0.07
MAT	-0.04	0.29	0.14	-0.19	0.20
Pancreas	0.04	0.05	0.09	-0.10	-0.25
SCAT	0.16	0.18	0.00	0.20	-0.39
Skin	-0.05	-0.23	0.44	0.00	0.38
Small	0.18	-0.01	-0.14	0.09	0.09
Spleen	-0.10	0.18	0.04	0.23	-0.58
WBC	-0.05	-0.06	0.53	-0.06	-0.17

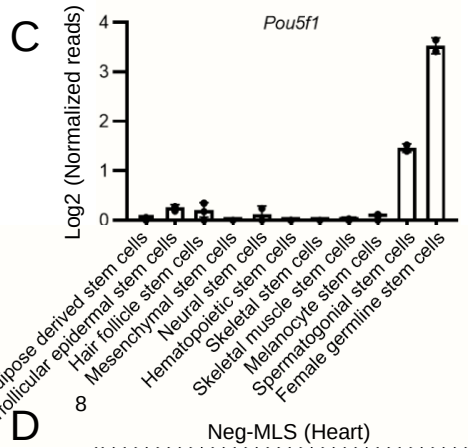

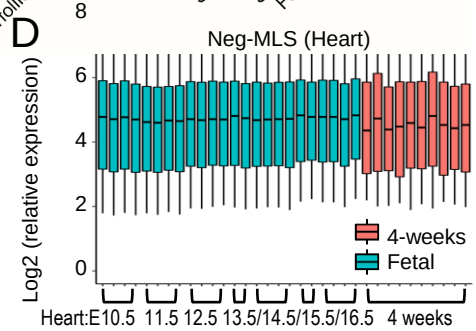

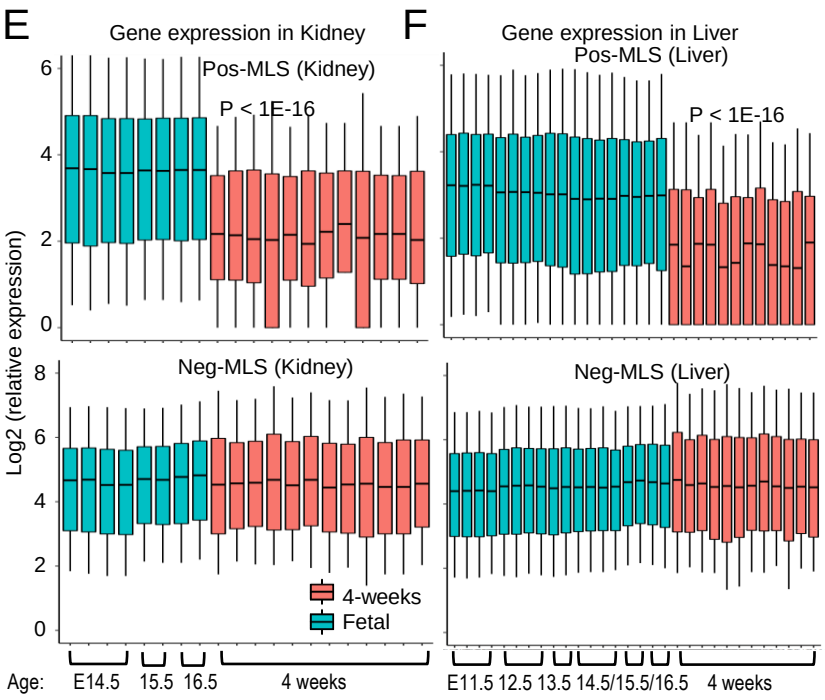

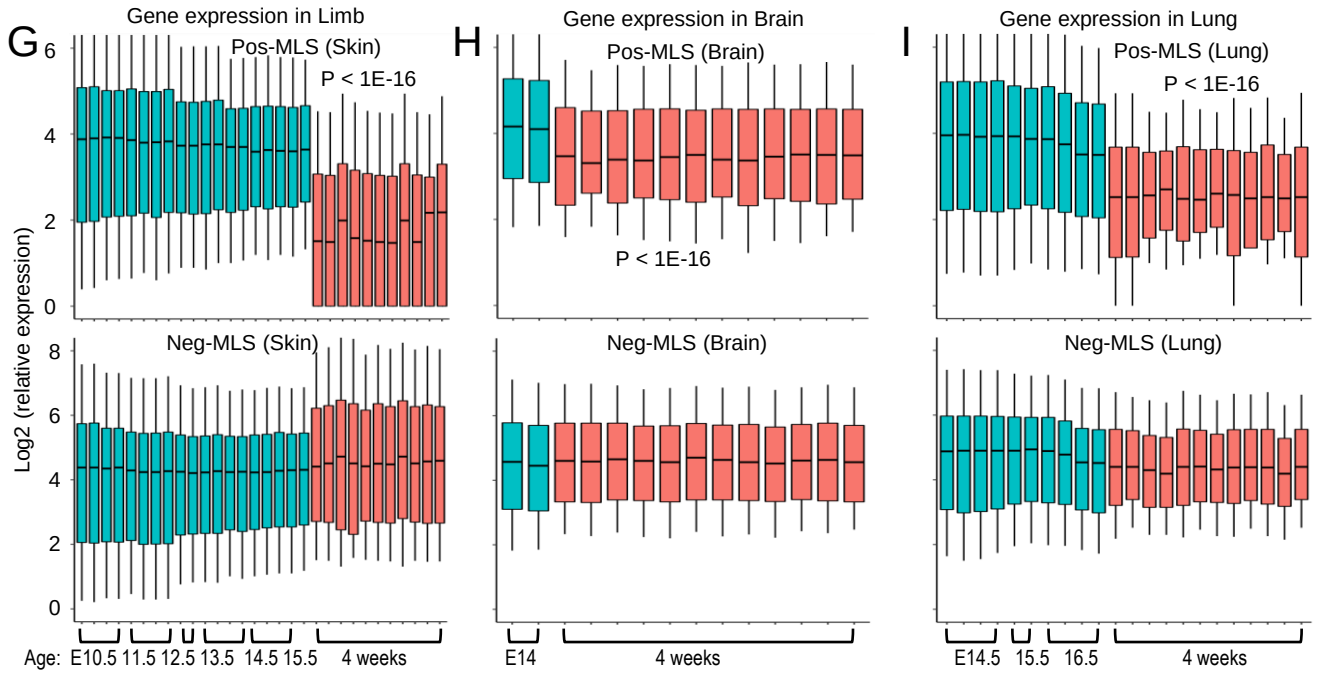

Figure S7. Differential expression of Pos-MLS genes between fetal and postnatal tissues. Related to Figure 7.

(A) Gene expression of *Pou5f1* in six tissues during aging. Raw reads were normalized by the Trimmed Mean of M-values method.

(B) Spearman correlation coefficients of gene expression with age across 17 tissues during aging.

(C) Barplot showing the gene expression of *Pou5f1* in adult stem cells.

(D) Boxplot showing the expression of Neg-MLS genes identified in the heart. Gene expression of the fetal heart is shown in light blue. Gene expression of the postnatal heart (4-weeks old) is shown in orange. p values were calculated using two-tailed Student's t-test.

(E-I) Boxplot showing the gene expression of Pos- and Neg-MLS genes identified in the Kidney (E), Liver (F), Skin (G), Brain (H) and Lung (I). Gene expression of fetal tissues is shown in light blue. Gene expression of the postnatal tissues (4-weeks old) is shown in orange. p values were calculated using two-tailed Student's t-test.